Characterization and Effect of Hydrogen Treatment and UV Irradiation on Photosensitive Sol−Gel Derived Aluminosilicate Planar Waveguides

J. M. Nedelec,*,† J. Grimblot,‡ S. Turrell,† and M. Bouazaoui§

Laboratoire de Spectrochimie Infrarouge et Raman, CNRS UMR 8516, Bât. C8, Laboratoire de Catalyse de Lille, UPRESA 8010, Bât. C3, and Laboratoire de Physique des Lasers, Atomes et Molécules, CNRS UMR 8523, Bât P5, Centre d'Etudes et de Recherches Laser et Applications, Université des Sciences et Technologies de Lille, 59655 Villeneuve d'Ascq Cedex, France

Received: August 4, 1999; In Final Form: October 30, 1999

Photosensitive Ce^{3+}-doped aluminosilicate planar waveguides have been prepared by a sol−gel process. The waveguides, which have been characterized using different techniques, appear to be totally amorphous and of good optical quality. The *m*-lines technique and waveguide Raman spectroscopy have shown that the doping of the guides with Ce^{3+} ions slows the densification process and that consequently the effect of doping has to be taken into account for the characterization of such materials. X-ray photoelectron spectroscopy (XPS) analysis of the samples has revealed a very high concentration of nonbridging oxygens (NBO) at the surface. To study the mechanisms responsible for the photosensitivity of these waveguides, selected samples have been hydrogenated and irradiated with UV light and then analyzed by XPS. Results have shown a strong decrease of the O/(Al + Si) atomic ratio, especially at the surface of these guides, after H_2 loading and UV irradiation. This decrease is correlated with the high concentration of NBO at the surface of the samples and has been interpreted as resulting from the formation of molecular water accompanied by the creation of defects in the glass.

1. Introduction

Over the past few years, there has been great enthusiasm for the study of passive and active planar waveguides because of their potential applications in the realization of integrated all-optical devices.[1−3] Among the materials used in optronics, photorefractive materials are of particular interest. In effect, one can induce a permanent variation of the refractive index in such materials by laser irradiation. If the irradiation is periodic in space, then the resulting modulation of the refractive index is also periodic and the final material acts as a Bragg grating. This effect, initially observed in germanosilicate optical fibers,[4] leads to a photoinduced refractive index change that offers potential applications in optical communications.[5] In recent years, the photorefractive effect has been observed in numerous other materials, including rare-earth-doped aluminosilicate fibers[6−8] and most recently, within our research group, in rare-earth-doped aluminosilicate planar waveguides.[9] In all cases, the preliminary exposition of the material to hydrogen has been shown to enhance the photorefractive effect.[10,11]

If the study of the photosensitivity of the different systems is quite well documented in the literature,[12] there is a recognized lack of understanding of the mechanisms responsible for the observed photosensitivity. However, a thorough understanding of these mechanisms is the key to the production of new materials with enhanced properties. Most of the studies devoted to the comprehension of the microscopic mechanisms have concerned germanosilicate glasses[13] because of their extensive use in telecommunications. In the present work, we examine Ce^{3+}-doped aluminosilicate planar waveguides.

Since the sol−gel method has been proven to be a suitable method for the preparation of homogeneous multicomponent glasses both as bulk materials and as thin films,[14,15] in the present work the waveguides were produced by combining sol−gel and dip-coating processes. The waveguides were first characterized by optical-loss measurements, *m*-lines techniques, and waveguide Raman spectroscopy (WRS) and X-ray photoelectron spectroscopy (XPS). The materials were then hydrogenated and irradiated, and changes at each step were investigated by XPS.

2. Experimental Section

2.1. Waveguide Elaboration. The procedure for the preparation of aluminosilicate planar waveguides has been already detailed elsewhere.[14,16] Briefly, a silicon sol is prepared by hydrolysis of tetraethyl orthosilicate in an acidic alcoholic medium. This sol is mixed with an aluminum sol prepared by dissolving aluminum tri-*sec*-butoxide in alcohol. The amounts of reagents were chosen to obtain a molar ratio of $x = Al/Si = 2$, which was kept constant throughout the study. The final sol was doped with Ce^{3+} ions by adding hydrated cerium nitrate salt ($Ce(NO_3)_3 \cdot 6H_2O$). The concentration of cerium (Ce/(Al + Si) molar ratio) varied from 0 to 2%. The resulting solution was then used in a dip-coating process.[17]

The substrates were either optical grade 25 mm × 75 mm × 1 mm Suprasil slides or monocrystalline silicon wafers coated with 2 μm of silica deposited by plasma enhanced chemical vapor deposition (PECVD). The substrates were dipped and withdrawn from the coating solution at a constant rate of 40 mm/min. After each dip, the sample was treated at 650 °C, and after every five dips it was annealed at 900 °C for 1 h. This procedure allowed the densification of the films and the complete elimination of organic residues.

* To whom correspondence should be addressed. Permanent address: Dr. J. M. Nedelec, Laboratoire des Matériaux Inorganiques ESA 6002, Université Blaise Pascal, 24 Avenue des Landais, 63 177 Aubiere Cedex, France. E-mail: jnedelec@chimtp.univ-bpclermont.fr.

† Laboratoire de Spectrochimie Infrarouge et Raman.

‡ Laboratoire de Catalyse de Lille.

§ Laboratoire de Physique des Lasers, Atomes et Molécules.

10.1021/jp992767n CCC: $19.00
Published on Web 01/19/2000

TABLE 1: Labeling of the Samples Used for the Study of the Photosensitivity

name	doped 2% Ce^{3+}	H_2	UV
AlSi			
AlSiCe	×		
AlSiH2		×	
AlSiCeH2	×	×	
AlSiUV		×	×
AlSiCeUV	×	×	×

TABLE 2: Refractive Index (n_f) and Thickness (t) of One Undoped Waveguide and One Doped Waveguide Obtained after 30 Dipping Cycles

sample	n_f	t (nm)
undoped	1.548 ± 0.001	1080 ± 100
doped 1%	1.526 ± 0.002	1200 ± 30

2.2. Waveguide Characterization. The optogeometrical parameters (refractive index n and thickness t) were measured for multimode (two TE and two TM modes) waveguides with a standard m-lines setup[18,19] using the 632.8 nm line of a He−Ne laser. The optical losses were estimated by analysis of the light scattered by the waveguide[20] while guiding at 632.8 nm.

The amorphous structure of the waveguides was checked using waveguide Raman spectroscopy (WRS).[21,22] The waveguide mode was excited with an argon ion laser operating at 488 nm. The light was coupled into the waveguide with a high-refractive-index prism that was clamped to the film. The streak of the guided mode was then imaged onto the slits of a Dilor triple monochromator. The spectral resolution was approximately 1 cm^{-1}.

2.3. Photosensitivity of Waveguides. The study was carried out on six types of samples labeled in Table 1, where a cross indicates that the sample was submitted to the corresponding treatment. Half of the samples were undoped, while the others were doped at 2% with Ce^{3+} ions. Some of the samples were used as prepared, some were simply hydrogenated, and others were hydrogenated and irradiated under UV.

The hydrogenation was carried out by exposing the samples to a flow of a mixture of high-purity H_2 and N_2 gases (H_2 /N_2 = 10%) at 450 °C for 2 h. This heat-treatment hydrogenation was chosen rather than high-pressure room-temperature hydrogenation, in accord with previous results obtained within our group for sol−gel derived germanosilicate glasses.[23] These results showed that high-pressure hydrogen loading at room temperature, which is the usual procedure used for fibers, is not efficient for similar sol−gel derived planar waveguides. However, a treatment under flowing hydrogen at higher temperatures leads to a great enhancement of the photorefractive effect in these waveguides.

For samples $AlSiH_2$ and $AlSiCeH_2$, the hydrogenation was performed directly in the XPS spectrometer chamber in order to prevent any further contact with air. Samples AlSiUV and AlSiCeUV were hydrogenated in a tubular oven and irradiated immediately afterward. A pulsed excimer-pumped frequency-doubled dye laser (λ = 244 nm) was used for the irradiation. The laser beam was focused into an afocal spherical telescope. The sample was then positioned in the telescope so that its position determined the size of the laser spot. Following previous results,[9] in the present work we used fluences of 150 mJ/cm^2 corresponding to a spot of 0.5 mm^2. The number of pulses was 30 000 with a repetition rate of 10 Hz.

For this study, the waveguides were deposited on silica slides. The irradiated zone was identified by painting the back-side of the sample with ink. The UV light passing through the sample ablated the ink; hence, the irradiated zone corresponding to the nonpainted zone was easily identified within the XPS spectrometer. This method is very simple and efficient, and since the ink is not on the side to be analyzed, no deleterious interaction among the sample, ink, and UV light is possible.

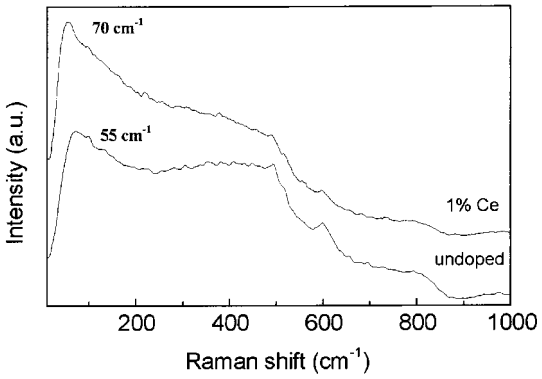

Figure 1. Waveguide Raman spectra for one undoped and one 1% Ce^{3+}-doped waveguides anealed at 900 °C.

X-ray photoelectron spectra were recorded using a VG Scientific 220XL Escalab. The X-ray source was the monochromatized Kα radiation of aluminum (1486.6 eV) operating with a spot diameter of 150 μm in order to be sure to analyze only the irradiated zone. The analyzer functioned in a constant-pass energy mode of 50 eV using the magnetic mode facility. Because of the insulating nature of the samples, an electron flood gun source of 6 V was applied to the samples during analysis to compensate the charging effect. The pressure in the analysis chamber was less than 10^{-9} mbar, and the binding energy scale was referenced on the position of the adventitious carbon C 1s line at 285 eV. Depth profiles were performed using an Ar^+ ion beam with the following experimental parameters: argon gas pressure of 2×10^{-7} mbar, ion energy of 3 keV, and ion current of 1 μA.

3. Results

3.1. Waveguide Characterization. The measured optical losses varied from 0.2 to 1 dB/cm, the former being the detection limit of our setup. The value of the optical losses was found to depend appreciably on the quality of the sample and on the conditions of deposition. Nevertheless, the values obtained for the best waveguides are very satisfactory for potential applications. However, it has been shown that there is a clear trend for the optical losses to increase when the guides are doped with Ce^{3+} ions.

The optogeometric parameters for two waveguides, one undoped and the other doped at 1% with Ce^{3+} ions, are shown in Table 2. These multimode waveguides were both obtained with cycles of 30 dips.

The values obtained for other Ce^{3+} concentrations do not differ very much from these. One observes a clear effect of the doping on the optogeometrical parameters of these waveguides. Since the doped waveguide is much thicker than the undoped one, it follows that the doped sample is less densified. In accordance, one can note a resulting lower refractive index for this sample.

To study the structural changes resulting from the doping with cerium ions, WRS was employed because it has been shown to be a very useful tool for the study of amorphous thin films.[22,24] The WRS spectra obtained for undoped and 1% doped sample are shown in Figure 1.

The spectra obtained are typical of totally amorphous aluminosilicate materials. The same vibrational bands are observed

TABLE 3: XPS Results of the Surface of the Waveguides with Different Concentrations of Ce^{3+} Ions

sample	Al/Si ± 0.02	O/(Al + Si) ± 0.02
undoped	1.44	2.02
0.5% Ce	1.51	2.04
1% Ce	1.75	2.02
2% Ce	1.76	2.06

TABLE 4: Bulk Composition of the Different Films

sample	Al/Si ± 0.02	O/(Al + Si), ±0.02	Ce/(Al + Si), ±0.004
AlSi	2.67	1.7	
AlSiH2	3.00	1.46	
AlSiUV	2.82	1.38	
AlSiCe	3.04	1.49	0.030
AlSiCeH2	2.80	1.47	0.030
AlSiCeUV	2.85	1.43	0.030

in both spectra, but they are well resolved in the spectra of the doped samples. This is particularly obvious for the bands at 490 and 606 cm^{-1}, which are attributed to four- and three-membered rings in the vitreous matrix, respectively. The intense feature observed in the low-frequency range is called the Boson peak and is characteristic of the vitreous structure. This peak located at 70 cm^{-1} for the undoped sample shifts to 55 cm^{-1} for the doped one. The spectra for the other cerium concentrations (0.5% and 2%) are similar to that of the 1% doped sample.

The XPS characterization of these waveguides has been presented elsewhere.[16] These studies showed that the waveguides were homogeneous and that the cerium ions exist exclusively in the +3 oxidation state. In this paper, we will focus on the oxygen concentration at the surface of the waveguides. The atomic ratios of aluminum to silicon, Al/Si, and of oxygen to aluminum and silicon, O/(Al + Si), are shown in Table 3 for the different samples.

The Al/Si ratios are shown because they will be used in further calculations and in the discussion section. The O/(Al + Si) ratio is constant for all the waveguides.

3.2. Effect of H_2 Loading and UV Irradiation. The data derived from the XPS depth profiles for the different samples are displayed in Table 4.

Figure 2 shows typical profiles obtained for an undoped (a) and a doped waveguide (b). The ratios have been calculated in the zone of constant profile corresponding to the major part of the samples. We observe a decrease of the O/(Al + Si) ratio after hydrogenation and UV irradiation for both doped and undoped samples. This decrease is much greater at the surface of the samples as shown in Table 5. But while it appears that hydrogenation and UV irradiation provoke a diminution of the oxygen concentration, especially at the surface of the guides, the cerium doping does not seem to have any effect on this phenomenon.

4. Discussion

4.1. Characterization of Waveguides and Effect of Doping with Ce^{3+}. *4.1.1. "m-Lines" and WRS Results*. The "*m*-lines" results indicate that the doped waveguides are less dense than the undoped one (Table 2). Low-frequency Raman analysis supports this conclusion. In effect, the shift of the Boson peak (BP) to lower frequency for the doped samples can be interpreted as a negative effect of the doping on the densification. This effect is similar to that of Mn^{2+} doping in silica xerogels, which we recently reported.[25] It has been demonstrated that the BP results from a maximum in the vibrational density of states (VDOS). According to the noncontinuous model of vitreous structure proposed by Duval et al.,[26] this maximum of VDOS is related to vibrations localized within cohesive domains constitutive of the glass. The position of the BP is related to the size of the cohesive domains, and the profile of the peak reflects the size distribution. The typical evolution of the BP along the densification process is toward higher frequencies, corresponding to an increase of the structural disorder and a decrease of the mean size of the cohesive domains. It results from these observations that the shift to lower frequencies of the BP for the doped samples indicates hindering of the densification process and the existence of larger cohesive domains in these samples.

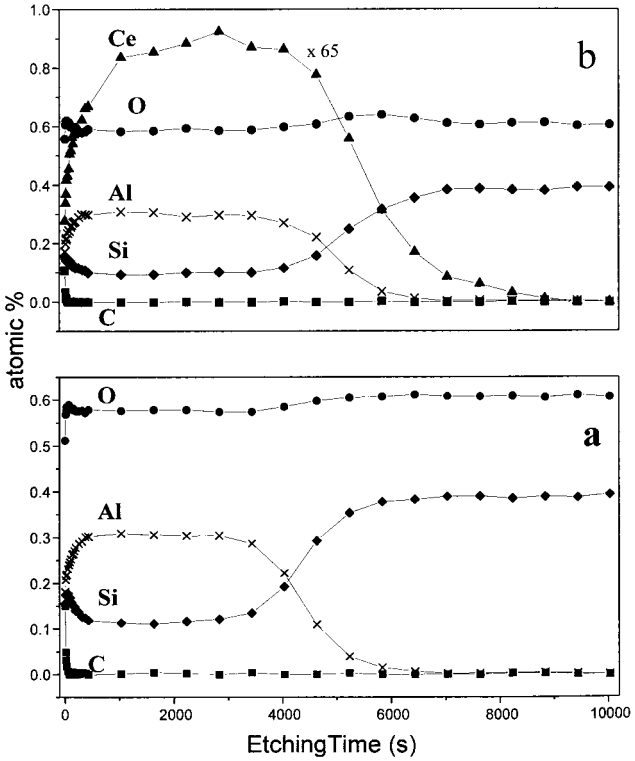

Figure 2. XPS profiles for (a) an undoped waveguide and (b) a Ce-doped waveguide.

TABLE 5: Composition of the Films at Their Surface

sample	O/(Al + Si) ±0.02
AlSi	2.02
$AlSiH_2$	1.72
AlSiUV	1.53
AlSiCe	2.06
$AlSiCeH_2$	1.67
AlSiCeUV	1.48

4.1.2. X-ray Photoelectron Spectroscopy Results. We recall that all waveguides, considering the experimental procedure used, have the nominal composition $Al_2O_3-SiO_2$ corresponding to atomic ratios Al/Si = 2 and O/(Al + Si) = $^5/_3$. Nevertheless, results of Table 3 show that at the surface of the waveguides this nominal composition Al/Si = 2 is not attained.

Given x = Al/Si, the theoretical atomic ratio O/(Al + Si) is given by

$$\frac{O}{Al+Si}=\frac{\frac{3}{2}x+2}{x+1} \qquad (1)$$

Hence, for 1.76 > x > 1.44 (see Table 3), the ratio O/(Al +

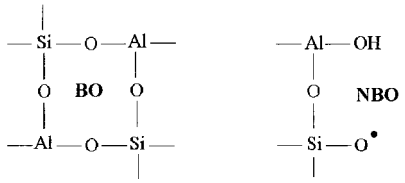

Figure 3. Bridging and nonbridging oxygens in an aluminosilicate glass.

TABLE 6: Percentage of Oxygen (% O) and of NBO (*y*) for the Surfaces of the Different Waveguides

% Ce	O/(Al + Si)	*x*	% O	*y*
0	2.02	1.44	0.669	0.185
0.5	2.04	1.51	0.671	0.201
1	2.02	1.75	0.669	0.201
2	2.06	1.76	0.673	0.225

Si) varies between 1.68 and 1.71. These values are always inferior to the observed value of 2. There is consequently an excess of oxygen at the surface of the waveguides with respect to the nominal stoichioemetry. This excess can be interpreted as being due to an important concentration of nonbridging oxygen at the surface of the waveguides. These nonbridging oxygens (NBO) are not fully integrated in the glass network by opposition to bridging oxygen (BO). These NBO are very numerous, for example, in alkaline silicate glasses and are responsible for the low melting temperature of these glasses. In effect, the presence of NBO provokes a decrease of the cohesion of the glass network. The differences between NBO and BO are shown in Figure 3. The NBO can correspond to hydroxyl groups or isolated oxygen defects. This assumption on the presence of NBO is supported by recent work of Stebbins and Xu,[27] who showed that for Ca-containing aluminosilicate glasses, the concentration of NBO, as derived from NMR spectra, is very high and reaches 5% in the bulk material.

If we call *y* the percentage of NBO, the total number of oxygens per mole of glass is then

$$2(1+y)+\frac{3}{2}x(1+y)$$

The first term is due to NBO linked to Si atoms and the second one to Al atoms. Consequently, the percentage of oxygen in the guide is given by

$$\%\,\mathrm{O}=\frac{\left(2+\frac{3}{2}x\right)(1+y)}{(1+x)+\left(2+\frac{3}{2}x\right)(1+y)} \qquad (2)$$

From eq 2, we can derive

$$y=\frac{(1+x)(\%\,\mathrm{O})-\left(2+\frac{3}{2}x\right)(1-\%\,\mathrm{O})}{\left(2+\frac{3}{2}x\right)(1-\%\,\mathrm{O})} \qquad (3)$$

Using eq 3, we find the results shown in Table 6.

The calculated concentration of NBO at the surface of the guides is very high and is probably due to the presence of numerous Al−OH and Si−OH groups. It is also worthy to note that doping with Ce^{3+} ions tends to increase the concentration of NBO.

4.2. Hydrogenation and UV Irradiation of Samples. The decrease of oxygen concentration in the waveguides, when conditions of Bragg grating inscription (H_2 + UV) are used,

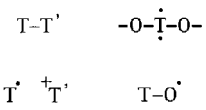

Figure 4. Defects in the aluminosilicate glass structure.

can be interpreted in the following way:

$$\mathrm{Si{-}OH}+\mathrm{HO{-}Si}\xrightarrow{\mathrm{H_2+UV}}\mathrm{H_2O}+\mathrm{Si^{\bullet}}+\mathrm{Si{-}O^{\bullet}}$$

The NBO present in the glass react together to form molecular water. This water is then eliminated in the vacuum of the XPS spectrometer (in this equation, silicon atoms may be replaced by aluminum ones).

This formation of water has already been postulated, and recently, Cordier et al. demonstrated its formation in germanosilicate and aluminosilicate preforms after hydrogenation and irradiation with UV light.[28] The formation followed by elimination of water molecules would then lead to a decrease of the O/(Al + Si) ratio as observed. The enhancement of this phenomenon at the surface of the samples could be due to the high concentration of NBO. The creation of water results in the appearance of defects in the glass structure. Such defects have been identified and classified for silica and can be extended to aluminosilicate glasses as shown in Figure 4. T and T′ stand for either a silicon or an aluminum atom, and the point for a single electron. These defects can then act as precursors for the observed photosensitivity. Since some of these defects are paramagnetic, they could be observed by ESR spectroscopy. The creation of such defects is also supported by experimental observations. In effect, the neutralization of the charging effect during the XPS experiments on AlSiUV and AlSiCeUV samples was found to be difficult to establish in a steady way. This difficulty appeared very localized in the irradiated zone, and this electrical perturbation could be due to the existence of the preceding defects.

5. Conclusion

We have shown that the sol−gel process is a convenient way for producing photosensitive aluminosilicate planar waveguides with good optical quality. The characterization of these waveguides has led to the conclusion that doping with Ce^{3+} ions slows the densification process taking place in these materials. In particular, low-frequency Raman spectra indicated that Ce^{3+} ions hinders the densification, maintaining larger cohesive domains in the glass. X-ray photoelectron spectroscopy has shown that there is a large number of nonbridging oxygens (NBO) at the surface of the waveguides. The hydrogenation and UV exposure of the samples provoke a decrease of the O/(Al + Si) ratio especially at the surface of the guides. This decrease has been interpreted as resulting from the creation of water molecules from the surfacic NBO.

Acknowledgment. The authors gratefully acknowledge Pr. M. Douay for helpful discussions and for the use of the excimer laser. The authors also thank L. Gengembre for his expert use of the XPS spectrometer. The Centre d'Etudes et de Recherche Lasers et Applications (CERLA) is supported by the Ministère de l'Education Nationale de l'Enseignement Supérieur et de la Recherche, the Région Nord/Pas de Calais, and the Fonds Européen de Développement Economique des Régions.

References and Notes

(1) Stegeman, G. I; Stolen, R. H. *J. Opt. Soc. Am. B* **1989**, *6*, 652.

(2) Afonso, C. N.; Ballesteros, J. M.; Gonzalo, J.; Righini, G. C.; Pelli, S. *Appl. Surf. Sci.* **1996**, *96*−*98*, 760.
(3) Duverger, C.; Turrell, S.; Bouazaoui, M.; Tonelli, F.; Montagna, M.; Ferrari, M. *Philos. Mag. B* **1998**, *77*, 363.
(4) Hill, K. O.; Fujii, Y.; Johnson, D. C.; Kawasaki, B. S. *Appl. Phys. Lett.* **1978**, *32*, 647.
(5) Kringlebotn, J. T.; Archambault, J. L.; Reekie, L.; Payne, D. N. *Opt. Lett.* **1994**, *19*, 2101.
(6) Dong, L.; Wells, P. J.; Hand, D. P.; Payne, D. N. *J. Opt. Soc. Am. B* **1993**, *10*, 89.
(7) Dong, L.; Archambault, J. L.; Reekie, L.; Russell, J.; Payne, D. N. *Opt. Lett.* **1993**, *18*, 861.
(8) Broer, M. M.; Cone, R. L.; Simpson, J. R. *Opt. Lett.* **1991**, *16*, 1391.
(9) Nedelec, J. M.; Benatsou, M.; Bouazaoui, M.; Xie, W.; Douay, M.; Turrell, S. Proceedings of the 9th CIMTEC, Florence, Italy, June 1998; CIMTEC; p 585.
(10) Lemaire, P. J.; Atkins, R. M.; Mizrahi, V.; Reed, W. A. *Electron. Lett.* **1993**, *29*, 11919.
(11) Taunay, T.; Bernage, P.; Douay, M.; Xie, W. X.; Martinelli, G.; Niay, P.; Bayon, J. F.; Delevaque, E.; Poignant, H. *J. Opt. Soc. Am. B* **1997**, *14*, 1.
(12) Poumellec, B.; Kherbouche, F. *J. Phys. III* **1996**, *6*, 1595.
(13) Awazu, K.; Greene, B. I. *J. Non-Cryst. Solids* **1996**, *201*, 267.
(14) Benatsou, M.; Capoen, B.; Bouazaoui, M.; Tchana, W.; Vilcot, J. P. *Appl. Phys. Lett.* **1997**, *71*, 4288.
(15) Brusatin, G.; Guglielmi, M.; Martucci, A. *J. Am. Ceram. Soc*. **1997**, *80*, 3139.
(16) Nedelec, J. M.; Gengembre, L.; Turrell, S.; Bouazaoui, M.; Grimblot, J. *Appl. Surf. Sci*. **1999**, *142*, 243.
(17) Klein, L. C. *Sol*−*gel optics and applications*; Kluwer Academic Publishers: New York, 1994.
(18) Ulrich, R.; Torge, R. *Appl. Opt.* **1973**, *12*, 2901.
(19) Hunsperger, R. G. *Integrated Optics: theory and technology*; Springer Verlag: Berlin 1982.
(20) Okamura, Y.; Yoshinaka, S.; Yamamoto, S. *Appl. Opt.* **1983**, *22*, 3892.
(21) Swalen, J. D.; Santo, R.; Tacke, M.; Fisher, J. *IBM J. Res. Dev.* **1977**, *21* 168.
(22) Duverger, C.; Nedelec, J. M.; Benatsou, M.; Bouazaoui, M.; Capoen, B.; Ferrari, M.; Turrell, S. *J. Mol. Struct.* **1999**, *480*−*481*, 169.
(23) Razafimahatra, A. D.; Benatsou, M.; Bouazaoui, M.; Xie, W. X.; Mathieu, C.; Dacosta, A.; Douay, M. *Opt. Mater*., submitted.
(24) Mugnier, J.; Urlacher, C.; Plenet, J. C.; Champagnon, B. *J. Raman Spectrosc.* **1997**, *28*, 989.
(25) Nedelec, J. M.; Bouazaoui, M.; Turrell, S. *J. Non-Cryst. Solids* **1999**, *243*, 209.
(26) Duval, E.; Boukenter, A. T. *J. Phys.: Condens. Matter* **1990**, *2*, 10227.
(27) Stebbins, J. F.; Xu, Z. *Nature* **1997**, *390*, 60.
(28) Cordier, P.; Dalle, C.; Depecker, C.; Bernage, P.; Douay, M.; Niay, P.; Bayon, J. F.; Dong, L. *J. Non-Cryst. Solids* **1998**, *244*, 277.